The Ekman Vertical Velocity in an Enclosed β-Plane Ocean[1]

W. Lawrence Gates

The Rand Corporation
Santa Monica, California

ABSTRACT

The vertical flux beneath the surface boundary layer is determined by balancing the divergence induced in this layer by the prescribed wind stress and surface temperature with the divergence of an assumed geostrophic interior flow. In this manner the equilibrium surface height over an enclosed basin is formulated as a boundary-value problem, the solution of which leads directly to the Ekman vertical velocity. The corresponding vertical velocity at the top of the boundary layer over a level bottom is also determined. Under idealized conditions, the solutions for Ekman vertical velocity (dependent upon wind stress and vertical eddy viscosity) appear to be reasonable approximations to oceanic upwelling, particularly when the surface thermal forcing is considered; but solutions for more realistic conditions are needed to confirm this. For a specified zonal surface stress and temperature, intense vertical velocity (with a magnitude of the order of 10^{-3} cm sec^{-1}) is confined to within about 100 km of the western shore of the basin. In further studies of the circulation in the ocean's interior, the formulation may be of use in the prescription of boundary values on the vertical velocity.

1. *Introduction.* The action of surface wind stress on an underlying ocean has been extensively studied since the pioneering investigation by Ekman (1905). The characteristic depth of penetration by wind-induced motion (Ekman depth) depends upon both the vertical eddy diffusion and the Coriolis parameter; the net transport in deep water is normal to the imposed surface stress, with the horizontal velocity displaying the well-known spiral structure. The modification of these features in shallow water and near coastlines were also explored by Ekman, who introduced a bottom boundary layer whose transport complements that of the surface layer. In addition to describing the horizontal transport in terms of the wind stress, the Ekman theory provides an estimate of the net vertical flux required beneath the surface boundary layer by mass continuity. This is the so-called Ekman vertical velocity,

1. This research was supported by the National Science Foundation under contract C-415.
Accepted for publication and submitted to press 12 October 1968.

$$w_E = \frac{1}{\varrho_0 f} curl_z \pi^w, \tag{1}$$

where ϱ_0 is the (uniform) density, f is the (constant) Coriolis parameter, and $curl_z \pi^w$ is the local vertical (z) component of the curl of the wind-stress vector, π^w. Downward motion is thus associated with convergence in the surface layer.

The application of the Ekman theory on an oceanic scale, however, has been restricted by neglect of the latitudinal variation in the Coriolis parameter or β effect as well as by its formulation as a local problem rather than a boundary-value problem. The importance of the β effect was first pointed out by Sverdrup (1947), when he noted that the divergence of the interior flow is capable of compensating that of the wind-induced motions in the surface layer. (A bottom boundary layer therefore need not be introduced for this purpose.) This led to the familiar "wind-stress curl" relationship,

$$\beta \frac{\partial \psi}{\partial x} = \frac{1}{\varrho_0} curl_z \pi^w, \tag{2}$$

where $\partial\psi/\partial x$ is the eastward derivative of the (geostrophic) streamfunction, ψ (for the vertically integrated transport), and where $\beta = \partial f/\partial y$ is the northward derivative of f. This relationship gives a good approximation to the average large-scale meridional currents in the open ocean, but it was not until this relationship was reformulated as a boundary-value problem, with the addition of frictional effects, that a satisfactory representation of the complete circulation in a basin was obtained, including the characteristic westward intensification (Stommel 1948). A relationship essentially equivalent to (1) and (2) has been applied by Yoshida and Mao (1957) to large-scale upwelling, but the important effects of coastal boundaries were not considered.

The first purpose of this paper is to extend the relationship (1) to include the β effect in a formulation applicable to an enclosed ocean. The second purpose is to examine the modifications of this Ekman vertical velocity introduced by a prescribed temperature field (thermal forcing) at the surface. Both of these effects have recently been touched upon by Robinson (1965), and his approach to the problem will form a convenient framework for the analysis.

2. *Basic Equations and Boundary-layer Solutions for a Homogeneous Ocean.* Assuming steady motion and neglecting both inertial and lateral viscous effects in a homogeneous ocean, we write the equations of motion and continuity for the boundary layer,

$$-fv + \frac{1}{\varrho_0}\frac{\partial p}{\partial x} - A_v \frac{\partial^2 u}{\partial z^2} = 0, \tag{3}$$

$$fu + \frac{1}{\varrho_0}\frac{\partial p}{\partial y} - A_v\frac{\partial^2 v}{\partial z^2} = 0, \tag{4}$$

$$\frac{\partial u}{\partial x} + \frac{\partial v}{\partial y} + \frac{\partial w}{\partial z} = 0, \tag{5}$$

where p is pressure, u, v, and w are the velocity components along the eastward (x), northward (y), and upward (z) axes, respectively, A_v is the vertical eddy diffusivity (assumed constant), ϱ_0 is the (uniform) density, and $f = f_0 + \beta y$ is the Coriolis parameter on the β plane, with both f_0 and β considered constant. If $z = 0$ at the (level) bottom of the ocean of depth H, the boundary conditions accompanying (3) to (5) are

$$u = v = w = 0 \quad \text{at} \quad z = 0, \tag{6}$$

and

$$\frac{\partial (u, v)}{\partial z} = \frac{(\tau_x^w, \tau_y^w)}{\varrho_0 A_v}, w = 0 \quad \text{at} \quad z = H, \tag{7}$$

where τ_x^w and τ_y^w are the components of the tangential surface stress. In the interior, i.e., between the upper and lower boundary layers, the effects of vertical diffusion are considered negligible, and (3) and (4) reduce to statements of geostrophic flow independent of depth,

$$v_I = \frac{1}{f\varrho_0}\frac{\partial p}{\partial x}, \tag{8}$$

$$u_I = -\frac{1}{f\varrho_0}\frac{\partial p}{\partial y}; \tag{9}$$

but the continuity equation (5) implies a linear variation in w over (interior) depth

$$w_I = \left(\frac{\beta}{f^2\varrho_0}\frac{\partial p}{\partial x}\right)z + W, \tag{10}$$

where $W = W(x, y)$ is an arbitrary function to be determined.

The solutions for u and v within the boundary layers are readily obtained and, following Robinson (1965), they are written:

$$u = e^{-\zeta}(a \sin \zeta + b \cos \zeta), \tag{11}$$

$$v = e^{-\zeta}(a \cos \zeta - b \sin \zeta), \tag{12}$$

where ζ is a nondimensional boundary-layer coordinate defined below. We define the characteristic thickness E of an Ekman boundary layer as

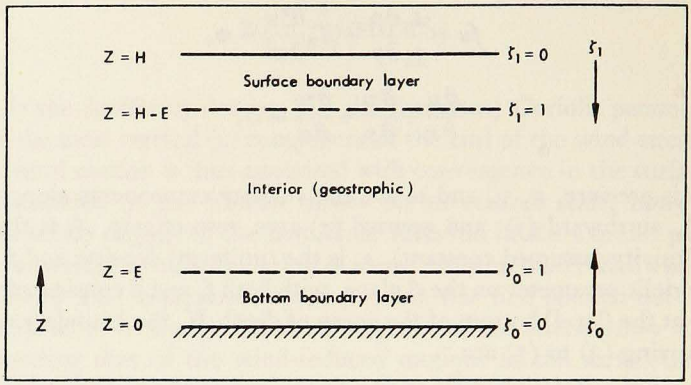

Figure 1. Boundary-layer identification and coordinates.

$$E = \left(\frac{2A_v}{f}\right)^{1/2}, \tag{13}$$

which[2] decreases with latitude on the β plane with the assumption of uniform A_v. In the surface boundary layer, say between $z = H - E$ and $z = H$, we have

$$\zeta = \zeta_1 \equiv \frac{H-z}{E}, \tag{14}$$

so that ζ_1 increases from 0 to 1 downward through the boundary layer, as sketched in Fig. 1. In this case the boundary condition (7) for u and v gives

$$a = (Ef\varrho_0)^{-1}(\tau_y^w - \tau_x^w), \tag{15}$$

$$b = (Ef\varrho_0)^{-1}(\tau_y^w + \tau_x^w). \tag{16}$$

In the bottom boundary layer, between $z = 0$ and $z = E$ (assuming A_v to be the same as in the surface layer), we have

$$\zeta = \zeta_0 \equiv \frac{z}{E}, \tag{17}$$

so that ζ_0 increases from 0 to 1 upward through the bottom boundary layer. Here the boundary condition (6) requires that $u(o) = -u_I$ and $v(o) = -v_I$, giving

$$a = -(f\varrho_0)^{-1}\frac{\partial p}{\partial x}, \tag{18}$$

2. This thickness is the depth at which the speed is reduced by the factor e^{-1} and is π^{-1} times the conventional Ekman depth.

$$b = (f\varrho_0)^{-1}\frac{\partial p}{\partial y}. \tag{19}$$

3. *Determination of the Vertical Velocity.* Following Robinson (1965), we now find the vertical velocity at the edges of the boundary layers by integration of the continuity equation, using the solutions (11) and (12) for u and v and applying the boundary condition $w = 0$ from (6) and (7). Hence, we obtain

$$\left.\begin{aligned} w(\zeta_1 = 1) \equiv w_1 &= \int_{H-E}^{H}\left(\frac{\partial u}{\partial x} + \frac{\partial v}{\partial y}\right)dz \\ &\simeq \frac{1}{\varrho_0}\,curl_z\left(\frac{\pi^w}{f}\right) \end{aligned}\right\} \tag{20}$$

and

$$\left.\begin{aligned} w(\zeta_0 = 1) \equiv w_0 &= \int_0^E\left(\frac{\partial u}{\partial x} + \frac{\partial v}{\partial y}\right)dz \\ &\simeq \frac{E}{2f\varrho_0}\left[\nabla^2 p - \frac{\beta}{2f}\left(\frac{\partial p}{\partial x} + \frac{\partial p}{\partial y}\right)\right] \end{aligned}\right\} \tag{21}$$

to the accuracy of the approximation that the depth of the boundary layers is small compared with the total depth of the ocean. On this same assumption we write, from (10),

$$w_I(z = H - E) \simeq w_I(z = H) = \frac{\beta H}{f^2\varrho_0}\frac{\partial p}{\partial x} + W, \tag{22}$$

and

$$w_I(z = E) \simeq w_I(z = 0) = W, \tag{23}$$

since the interior vertical velocity w_I changes relatively slowly in the vertical. We now equate the w_I of (22) and (23) to the w of (20) and (21), i.e., we require a matching of the boundary layer and interior solutions. Thus we find that

$$\frac{\beta H}{f^2\varrho_0}\frac{\partial p}{\partial x} + W - \frac{1}{\varrho_0}\,curl_z\left(\frac{\pi^w}{f}\right) = 0, \tag{24}$$

and

$$W - \frac{E}{2f\varrho_0}\nabla^2 p + \frac{E\beta}{4f^2\varrho_0}\left(\frac{\partial p}{\partial x} + \frac{\partial p}{\partial y}\right) = 0. \tag{25}$$

These results are equivalent to those of Robinson (1965).

Equations (24) and (25) are now regarded as two independent relationships for $p(x, y)$ and $W(x, y)$, and they may therefore serve to determine the interior

velocity distribution [(8) to (10)] in terms of the surface wind stress. Eliminating first W between (24) and (25), we have

$$E\nabla^2 p + \frac{\beta}{f}\left(2H - \frac{E}{2}\right)\frac{\partial p}{\partial x} - \frac{\beta E}{2f}\frac{\partial p}{\partial y} = 2\,curl_z \pi^w + \frac{2\beta\tau_x^w}{f}. \tag{26}$$

This determines the equilibrium pressure in terms of the wind-stress distribution and it explicitly displays the β effects. The presence of the terms in E constitutes a generalization of the Sverdrup relationship (2). Were $\beta = 0$, the pressure would be given by the Poisson equation

$$\nabla^2 p = \frac{2}{E} curl_z \pi^w. \tag{27}$$

This relationship, which was found by Ekman (1923) for the case of a deep ocean, has been extended by Welander (1957) to the case of shallow water. With $\beta = 0$, the vertical velocity at the base of the surface-boundary layer is given by

$$w_1 = W = \frac{1}{\varrho_0 f_0} curl_z \pi^w, \tag{28}$$

which is in agreement with (1); the interior vertical velocity (10) is uniform over depth, i.e., $w_I = w_0 = w_1 = W$.

Returning to (24) and (25) and eliminating p, we have

$$\frac{\partial W}{\partial x} - \frac{E}{2f\varrho_0}\left[\nabla^2 - \frac{\beta}{f}\left(\frac{\partial}{\partial x} + \frac{\partial}{\partial y}\right)\right]\left[\frac{f^2}{\beta H} curl_z\left(\frac{\pi^w}{f}\right) - \frac{\tau_x^w}{2H} - \frac{f^2\varrho_0 W}{\beta H}\right] = 0,$$

or, expanding and writing the β terms explicitly,

$$\left.\begin{aligned} E\nabla^2 W + \frac{\beta}{f}\left(2H - \frac{E}{2}\right)\frac{\partial W}{\partial x} + \frac{7\beta E}{2f}\frac{\partial W}{\partial y} + \frac{E\beta^2}{f^2} W = \frac{E}{\varrho_0 f}\nabla^2 curl_z \pi^w + \frac{\beta E}{f^2\varrho_0} \\ \times\left[\nabla^2(\tau_x^w) + \frac{1}{2}\frac{\partial}{\partial y}(curl_z \pi^w) - \frac{1}{2}\frac{\partial}{\partial x}(curl_z \pi^w)\right] \\ - \frac{\beta^2 E}{2f^3\varrho_0}\left(\frac{\partial \tau_x^w}{\partial x} + \frac{\partial \tau_y^w}{\partial x}\right). \end{aligned}\right\} \tag{29}$$

This equation serves to determine the function $W(x, y) = w_0$ in terms of the wind stress. In the case of $\beta = 0$, all terms except the first ones on the left-hand and right-hand sides vanish, and we recover (28).

Note that we cannot solve both (26) and (29) for p and W with independent prescriptions of lateral-boundary conditions, since the specification of boundary values for, say, p and the resultant pressure solution would presumably deter-

mine the solution as well as the boundary values for W through either (24) or (25). Which equation we solve is thus a matter of convenience, although the specification of boundary conditions is easier to justify physically in the case of (26). Here the condition p = constant corresponds to zero geostrophic flow normal to the lateral boundaries of the interior; this is a convenient assumption for the illustrative solutions shown below. Note, however, that this is not necessarily the correct boundary condition at the shore, and some modification of this constraint is discussed in § 7.

4. *Solutions for a Simplified Case.* The solution of (26) for the pressure distribution determines the interior horizontal flow through (8) and (9); and through (24) or (25) it permits determination of the vertical velocity W at the top of the bottom boundary layer. The interior vertical velocity is then found from (10). To illustrate the character of these solutions, consider the surface-stress field,

$$\left.\begin{aligned} \tau_x^w &= -T\cos\left(\frac{\pi y}{L}\right) \\ \tau_y^w &= 0, \end{aligned}\right\} \tag{30}$$

where L is the width of an assumed square ocean and T is the amplitude of the zonal stress. Consistent with the approximation $E \ll H$, we neglect both terms in βE on the left-hand side of (26), and, in addition, we neglect the term in β on the right-hand side. The latter approximation is valid where $curl_z \pi^w \gg \beta f^{-1}\tau_x^w$, as is the case over most of the basin, especially in the midlatitudinal zone of maximum stress curl; however, this approximation breaks down near the northern and southern boundaries in the present example. With these simplifications, (26) is written

$$\nabla^2 p + \gamma\frac{\partial p}{\partial x} = \frac{2}{E}curl_z \pi^w = -P\sin\left(\frac{\pi y}{L}\right), \tag{31}$$

where

$$\gamma = \frac{2\beta H}{Ef} \tag{32}$$

and

$$P = \frac{2T\pi}{EL}. \tag{33}$$

The requirement of zero geostrophic flow normal to the lateral boundary of the interior leads to the boundary condition $p = p_0$ = constant on $x = 0, L$ and $y = 0, L$. Regarding γ and P as constant, the solution of (31) is then written as

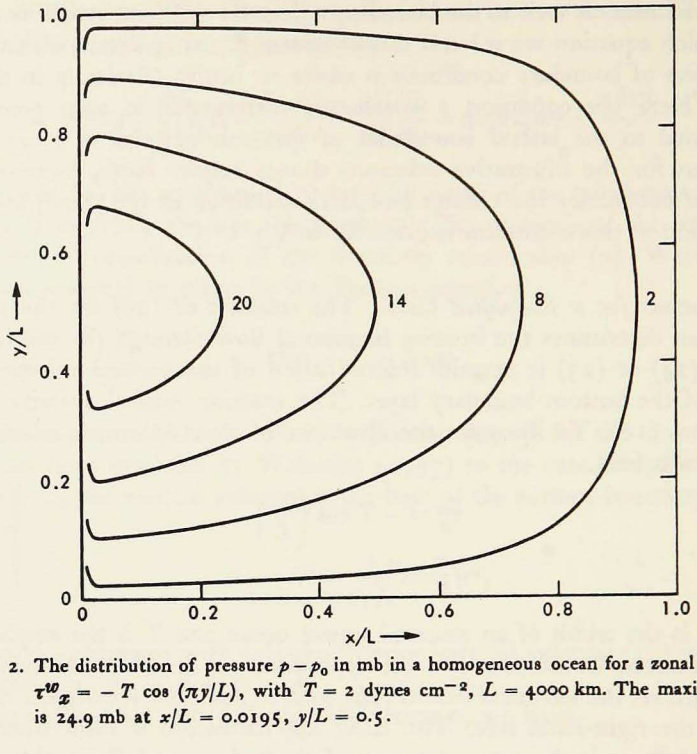

Figure 2. The distribution of pressure $p - p_0$ in mb in a homogeneous ocean for a zonal wind stress $\tau^w_x = -T \cos(\pi y/L)$, with $T = 2$ dynes cm^{-2}, $L = 4000$ km. The maximum $p - p_0$ is 24.9 mb at $x/L = 0.0195$, $y/L = 0.5$.

$$p - p_0 = -\frac{PL^2}{\pi^2} \sin\left(\frac{\pi y}{L}\right)\left[a_1 e^{b_1 x} + a_2 e^{b_2 x} - 1\right], \tag{34}$$

where

$$a_1 = (1 - e^{b_2 L})(e^{b_1 L} - e^{b_2 L})^{-1}, \tag{35}$$

$$a_2 = 1 - a_1, \tag{36}$$

and

$$b_{1,2} = -\frac{\gamma}{2} \pm \left(\frac{\gamma^2}{4} + \frac{\pi^2}{L^2}\right)^{1/2}. \tag{37}$$

This solution is analogous to that first given by Stommel (1948) for the steady wind-driven circulation in a rectangular ocean with bottom friction; (31) is structurally similar to the vorticity equation in this case, and the solution (34) displays the same pronounced zonal asymmetry that is familiar from Stommel's streamfunction solutions. The constant p_0 may be determined from the requirement of water mass conservation, $(\int_0^L \int_0^L p - p_0]\, dxdy = 0)$. For $T = 2$ dynes cm^{-2}, $L = 4000$ km, $H = 4$ km, f and β at 45°N, and $A_v = 150$cm^2 sec^{-1}, we find $E = 17.0$ m, $\gamma = 7.40 \times 10^{-7}$ cm^{-1}, and $P = 1.84 \times 10^{-11}$ dyne

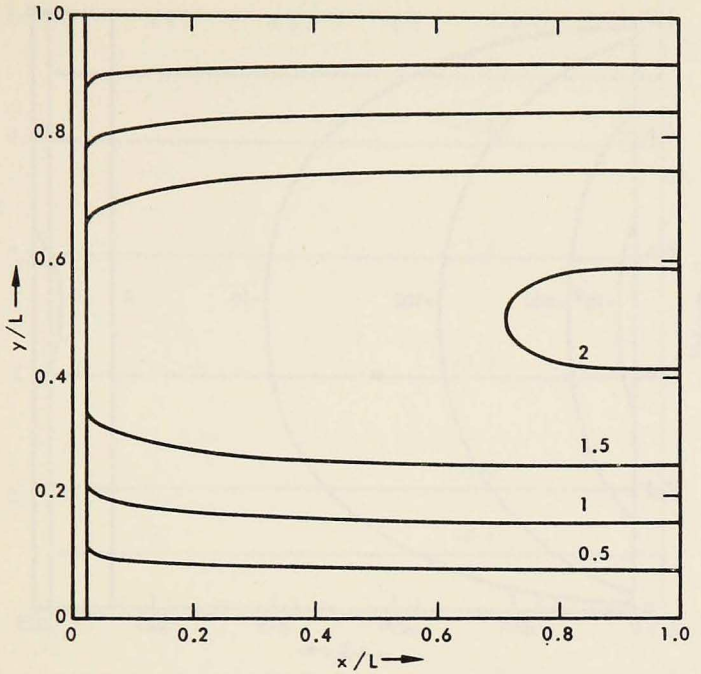

Figure 3. The distribution of vertical velocity $w_0 = W$ in 10^{-4} cm sec^{-1} at the top of the bottom boundary layer in a homogeneous ocean subject to a zonal surface wind stress. The value is zero on the lines $y/L = 0, y/L = 1$, and $x/L = 0.0217$; maximum upwelling of 2.07×10^{-4} cm sec^{-1} occurs at $x/L = 1, y/L = 0.5$. Downward motion is confined to a narrow zone along the western wall, details of which are shown in Fig. 4.

cm^{-4}. The solution (34) under these condition, shown in Fig. 2, displays a maximum pressure difference of about 25 mb near the western shore. As noted earlier, Fig. 2 serves as a streamline representation of the horizontal geostrophic interior motion between the boundary layers.

With $p - p_0$ now determined, we find from (22) the vertical velocity w_1 at the base of the surface boundary layer, once the distribution of the vertical velocity W at the top of the bottom boundary layer has been obtained. Returning to (25), therefore, and making use of (31) with the approximation $E \ll H$, we have

$$W = \frac{1}{\varrho_0 f} curl_z \pi^w - \frac{\beta H}{e_0 f^2} \frac{\partial p}{\partial x}, \tag{38}$$

which, with the solution (34) and the stress field (30), becomes

$$W = -\frac{T\pi}{Lfe_0} \sin\left(\frac{\pi y}{L}\right)\left[1 - \frac{2\beta HL^2}{fE\pi^2}(a_1 b_1 e^{b_1 x} + a_2 b_2 e^{b_2 x})\right]. \tag{39}$$

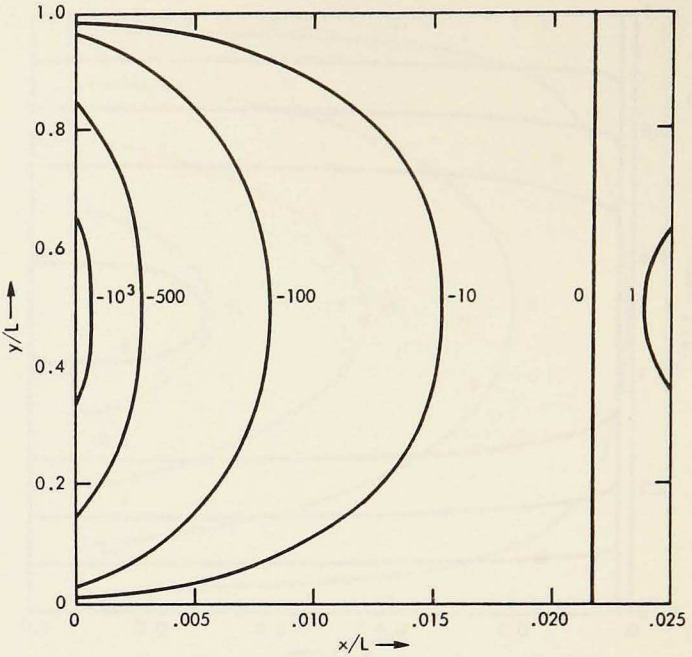

Figure 4. Detail of the distribution of vertical velocity W in 10^{-4} cm sec^{-1} in the region of sinking motion near the western boundary of Fig. 3. The maximum downward motion is -1132×10^{-4} cm sec^{-1} at $x/L = 0$, $y/L = 0.5$. Note the distortion of the x/L scale.

For the same constants used previously, this solution is shown in Figs. 3 and 4. The presence of β has here produced an intense sinking motion near the western boundary (with a maximum value of 1132×10^{-4} cm sec^{-1}) while a relatively weak rising motion occurs over most of the basin at this near-bottom level.

From (38) and (22) we find that the vertical velocity at the base of the surface boundary layer is simply

$$w_1 = \frac{1}{e_0 f} curl_z \pi^w. \tag{40}$$

For the stress (30), this distribution of w_1, shown in Fig. 5, represents only the convergence of the surface Ekman transport. In view of (10), this result implies that neglect of the variation of f in the last term of (24) is consistent with the neglect of the last term in the pressure equation (26); this returns us to the Ekman relationship (1). To this approximation, therefore, the vertical velocity beneath the surface layer is unaffected in the present model by the presence of lateral boundaries, on which both horizontal and vertical slip is permitted.

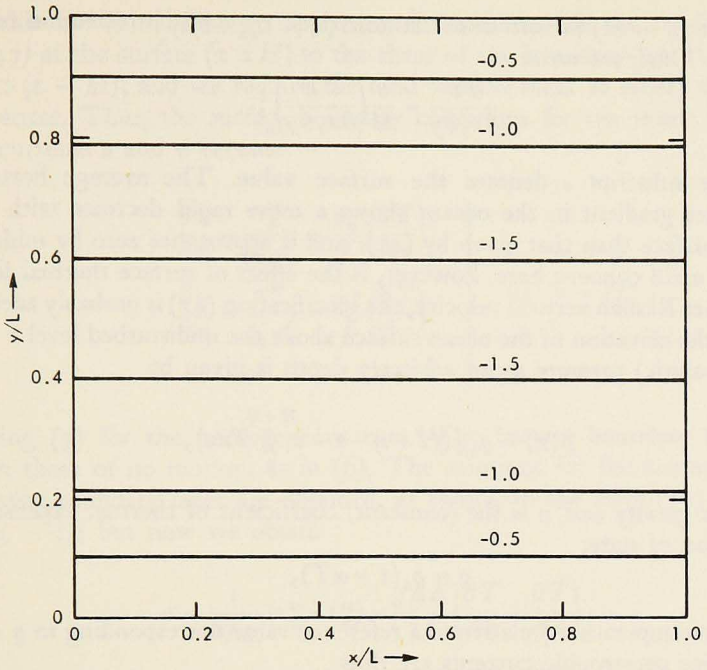

Figure 5. The distribution of vertical velocity w_1 in 10^{-4} cm sec^{-1} at the base of the surface boundary layer in a homogeneous ocean subject to a zonal wind stress $\tau^{w}{}_{x} = -T \cos(\pi y/L)$, with $T = 2$ dynes cm^{-2} and $L = 4000$ km. The vertical motion is given by $w_1 = -(T\pi/Lf\varrho_0) \sin(\pi y/L)$, with a maximum of -1.57×10^{-4} cm sec^{-1} at $y/L = 0.5$.

According to (10), the interior vertical velocity at intermediate levels ($E \leq z \leq H - E$) is given by a linear interpolation between the data in Figs. 3, 4, and 5. We may note that both the β term and the W term in (10) are of comparable size over most of the interior, while the β-induced sinking motion near the western shore is dominant immediately below the surface layer. In the absence of the β term (and hence for a nondivergent interior geostrophic motion), the vertical velocity would be that given for w_1 (Fig. 5) at all levels. This modification of the surface wind-induced divergence by the divergence of the interior motion is in the manner first suggested by Stommel (1956).

5. *The Case of a Nonhomogeneous Ocean.* The preceding analysis may be extended to include the effects of a surface temperature distribution on the Ekman vertical velocity. The prescribed temperature field is assumed to be maintained by surface-heat exchanges and to extend through the depth of the ocean in a manner consistent with the large-scale distribution of interior velocity. The simplest realistic assumption is that the magnitude of the horizontal temperature gradient decreases linearly with depth, from a maximum at

the surface ($z = H$) to zero at the bottom ($z = 0$), while its direction remains the same. Thus, we write

$$\frac{\partial T}{\partial x, \partial y} = \frac{z}{H}\left(\frac{\partial T}{\partial x, \partial y}\right)_0, \tag{41}$$

where the subscript $_0$ denotes the surface value. The average horizontal temperature gradient in the oceans shows a more rapid decrease with depth near the surface than that given by (41); and it approaches zero by midocean. Since our main concern here, however, is the effect of surface thermal forcing on the upper Ekman vertical velocity, the specification (41) is probably adequate.

If η is the elevation of the ocean surface above the undisturbed level $z = H$, the (hydrostatic) pressure at an arbitrary depth is given by

$$p(z) = \varrho_0 g(H + \eta - z - \alpha \int_z^{H+\eta} T dz), \tag{42}$$

where g is gravity and α is the (constant) coefficient of thermal expansion in the equation of state,

$$\varrho = \varrho_0(1 - \alpha T), \tag{43}$$

with T the temperature (relative to a reference value corresponding to $\varrho = \varrho_0$). The interior geostrophic currents are thus

$$u_I(z) = -\frac{1}{\varrho f}\frac{\partial p}{\partial y} = -\frac{g}{f}\frac{\partial \eta}{\partial y} + \frac{\alpha g(H^2 - z^2)}{2fH}\left(\frac{\partial T}{\partial y}\right)_0, \tag{44}$$

$$v_I(z) = \frac{1}{\varrho f}\frac{\partial p}{\partial x} = \frac{g}{f}\frac{\partial \eta}{\partial x} - \frac{\alpha g(H^2 - z^2)}{2fH}\left(\frac{\partial T}{\partial x}\right)_0, \tag{45}$$

where the approximations $\eta \ll H$ and $\varrho \simeq \varrho_0$ have been made when η and ϱ are undifferentiated. The presence of a temperature gradient thus permits the reversal of the current with depth. The (interior) shear,

$$\frac{\partial u_I}{\partial z} = -\frac{\alpha g}{fH}\left(\frac{\partial T}{\partial y}\right)_0 z, \tag{46}$$

$$\frac{\partial v_I}{\partial z} = \frac{\alpha g}{fH}\left(\frac{\partial T}{\partial x}\right)_0 z, \tag{47}$$

is a maximum near the surface and approaches zero at the bottom, so that the current shows relatively little variation with depth in the deeper water; this is in agreement with the observed structure of large-scale currents. In the absence of a surface temperature gradient, η becomes synonymous with p, and the geostrophic currents extend undiminished through the interior depth of the ocean, as in the homogeneous case.

Within the boundary-layer approximation we now add the conditions (46) and (47) at the surface ($z \simeq H$) to the shear of the boundary-layer currents at $\zeta_1 = 0$ ($z = H$), and we require the total vertical shear to satisfy the applied wind stress. Thus, the surface boundary conditions for the upper boundary-layer currents u and v become

$$\left.\begin{aligned} \frac{\partial u}{\partial z} &= \frac{\tau_x^w}{\varrho_0 A_v} + \frac{\alpha g}{f}\left(\frac{\partial T}{\partial y}\right)_0 \\ \frac{\partial v}{\partial z} &= \frac{\tau_y^w}{\varrho_0 A_v} - \frac{\alpha g}{f}\left(\frac{\partial T}{\partial x}\right)_0 \\ w &= 0 \end{aligned}\right\} \quad \text{at} \quad z = H, \tag{48}$$

replacing (7) for the homogeneous case. The bottom boundary conditions remain those of no motion, as in (6). The solutions for the currents within the upper boundary layer are obtained, as before, in the form (11) and (12), with $\zeta = \zeta_1$; but now we obtain

$$a = \frac{1}{Ef\varrho_0}(\tau_y^w - \tau_x^w) - \frac{g\alpha E}{2f}\left(\frac{\partial T}{\partial x} + \frac{\partial T}{\partial y}\right)_0, \tag{49}$$

$$b = \frac{1}{Ef\varrho_0}(\tau_y^w + \tau_x^w) - \frac{g\alpha E}{2f}\left(\frac{\partial T}{\partial x} - \frac{\partial T}{\partial y}\right)_0. \tag{50}$$

At $\zeta_0 = 0$, the boundary-layer speeds are $u(0) = b$ and $v(0) = a$; the interior speeds evaluated at $z = 0$ are, from (44) and (45), $u_I(0) = -gf^{-1}\,\partial\eta/\partial y + \alpha gH(2f)^{-1}(\partial T/\partial y)_0$ and $v_I(0) = gf^{-1}\,\partial\eta/\partial x - \alpha gH(2f)^{-1}(\partial T/\partial x)_0$. The requirement that the total horizontal velocity be zero at the bottom therefore gives

$$a = -\frac{g}{f}\frac{\partial\eta}{\partial x} + \frac{\alpha gH}{2f}\left(\frac{\partial T}{\partial x}\right)_0, \tag{51}$$

$$b = \frac{g}{f}\frac{\partial\eta}{\partial y} - \frac{\alpha gH}{2f}\left(\frac{\partial T}{\partial y}\right)_0, \tag{52}$$

with the solutions (11) and (12) in the lower boundary layer ($\zeta = \zeta_0$).

Applied to the interior flow, the continuity equation (5) gives

$$w_I(z) = -\int_0^z \left(\frac{\partial u_I}{\partial x} + \frac{\partial v_I}{\partial y}\right) dz + W, \tag{53}$$

where W is an arbitrary function to be determined. The use of (44) and (45) then gives

$$w_I(z) = \frac{\beta g}{f^2}\frac{\partial \eta}{\partial x} z - \frac{\beta \alpha g}{2 f^2 H}\left(\frac{\partial T}{\partial x}\right)_0 \left(H^2 z - \frac{z^3}{3}\right) + W. \tag{54}$$

The vertical velocity in this case varies as the cube of depth in the interior in contrast to the linear variation for the homogeneous case (10).

Integrating the continuity equation over the upper boundary layer from $\zeta_1 = 0$ to $\zeta_1 = 1$, using (11), (12), (49), and (50), and matching the resulting vertical velocity w_1 to the interior w_I (evaluated at $z = H$) from (54), we have

$$\left.\begin{aligned} &\frac{\beta g H}{f^2}\frac{\partial \eta}{\partial x} + W - \frac{\beta \alpha g H^2}{3 f^2}\left(\frac{\partial T}{\partial x}\right)_0 - \frac{1}{\varrho_0} curl_z\left(\frac{\pi^w}{f}\right) + \\ &\quad + \frac{g \alpha E^2}{2 f}\left(\nabla^2 T_0 - \frac{\beta}{f}\left(\frac{\partial T}{\partial y}\right)_0\right) = 0. \end{aligned}\right\} \tag{55}$$

This is the appropriate generalization of the homogeneous case (24) when $\partial p/\partial x = \varrho_0 g\, \partial \eta/\partial x$. Proceeding similarly for the lower boundary layer, we have

$$\frac{Eg}{2f}\nabla^2 \eta - W - \frac{g \beta E}{4 f^2}\left(\frac{\partial \eta}{\partial x} + \frac{\partial \eta}{\partial y}\right) - \frac{\alpha g H E}{4 f}\nabla^2 T_0 + \frac{\alpha g H \beta E}{8 f^2}\left(\frac{\partial T}{\partial x} + \frac{\partial T}{\partial y}\right)_0 = 0, \tag{56}$$

corresponding to (25) in the homogeneous case. Together with (55), this constitutes a system for the determination of the surface configuration η and of the (bottom) vertical velocity $w_0 = W$. The equation for $\eta(x, y)$ is readily found to be

$$\left.\begin{aligned} &E\nabla^2 \eta + \frac{\beta}{f}\left(2H - \frac{E}{2}\right)\frac{\partial \eta}{\partial x} - \frac{\beta E}{2 f}\frac{\partial \eta}{\partial y} \\ &\quad = \frac{2}{g \varrho_0} curl_z \pi^w + \frac{2 \beta \tau_x^w}{g f \varrho_0} + \alpha E\left(\frac{H}{2} - E\right)\nabla^2 T_0 \\ &\quad + \frac{\alpha \beta H}{f}\left(\frac{2H}{3} - \frac{E}{4}\right)\left(\frac{\partial T}{\partial x}\right)_0 + \frac{\alpha \beta E}{f}\left(E - \frac{H}{4}\right)\left(\frac{\partial T}{\partial y}\right)_0, \end{aligned}\right\} \tag{57}$$

which is a generalization of the homogeneous case (26). Solution of (57) permits the determination of W through either (55) or (56), and thence the determination of w_1 from (54). In the event that $\beta = 0$, (57) reduces to

$$E\nabla^2 \eta = \frac{2}{g \varrho_0} curl_z \pi^w + \alpha E\left(\frac{H}{2} - E\right)\nabla^2 T_0, \tag{58}$$

in which the effect of a local temperature excess ($\nabla^2 T_0 < 0$) is seen to be analogous to that of the *curl* of anticyclonic wind stress ($curl_z \pi^w < 0$). When $\beta = 0$, (55) becomes

$$W = \frac{1}{\varrho_0 f} curl_z \pi^w - \frac{g\alpha E^2}{2f} \nabla^2 T_0, \tag{59}$$

which is equivalent to a relationship previously given by Robinson (1965). In this case the imposition of a uniform temperature gradient has no effect on the surface height or on the vertical velocity distribution.

In considering the reduction of (57), we neglect, as before, the terms in $E\partial\eta/\eta x$ and $E\partial\eta/\partial y$ on the left-hand side, and we also neglect the term in $(\partial T/\partial y)_0$ in comparison to that in $(\partial T/\partial x)_0$ on the right-hand side, upon enforcement of the assumption that $E \ll H$. If we further neglect the term in τ_x^w, as was done in the corresponding homogeneous case, and if we assume that $(\partial T/\partial x)_0 = 0$, we have

$$E\nabla^2\eta + \frac{2\beta H}{f}\frac{\partial\eta}{\partial x} = \frac{2}{g\varrho_0} curl_z \pi^w + \frac{\alpha E H}{2} \nabla^2 T_0. \tag{60}$$

The solution of (60) for the zonal wind stress (30) and for the zonal surface temperature distribution

$$T_0(y) = \theta_0 - \frac{\Delta\theta}{L} y + \frac{\Delta\theta}{\pi} \sin\left(\frac{\pi y}{L}\right) \tag{61}$$

is given by

$$\eta - \eta_0 = \frac{-L^2}{\pi^2}\left(\frac{P}{\varrho_0 g} + Q\right) \sin\left(\frac{\pi y}{L}\right)[a_1 e^{b_1 x} + a_2 e^{b_2 x} - 1], \tag{62}$$

where

$$Q = \frac{\alpha H \pi \Delta\theta}{2L^2}. \tag{63}$$

Here θ_0 and $\Delta\theta$ are constants, and η_0 is a constant to insure zero interior geostrophic flow normal to the boundary; η_0 is given by

$$\eta_0 = \frac{2L}{\pi^3}\left(\frac{P}{\varrho_0 g} + Q\right)\left[\frac{a_1}{b_1}(e^{b_1 L} - 1) + \frac{a_2}{b_2}(e^{b_2 L} - 1) - L\right] \tag{64}$$

from the requirement of conservation of total water mass.

When $\Delta\theta = 20$ deg and $\alpha = 2.5 \times 10^{-4}$ deg^{-1} and when the previous constants are used, $Q = 1.9 \times 10^{-14}$cm^{-1} and $P/\varrho_0 g = 1.8 \times 10^{-14}$cm^{-1}. Under these conditions, the thermal contribution to the pressure distribution is comparable to the wind-induced portion, and the two reinforce each other in the present case. The solution (62) for η, which is, in fact, proportional to the solution (34) for the pressure in the homogeneous case, is given in Fig. 2, with the isoline conversion 1 mb pressure = 1 cm elevation. The Ekman vertical velocity w_1 at the base of the surface boundary layer is likewise pro-

portional to that of the homogeneous case (40). Fig. 5, therefore, also describes w_1 for the present case when the magnitudes are increased by the factor $(1 + Q\varrho_0 g/P) = 2.0$.

6. *The Estimation of Upwelling.* Although it is clear that a wide variety of stress and surface-temperature distributions could be considered, the above example is sufficient to show that the thermal contribution in the present formulation is comparable to that of the surface stress. Moreover, the solutions for the Ekman vertical velocity W display a magnitude and coastal confinement similar to that of the average large-scale upwelling in the middle latitudes, which is characteristically confined to a few hundred kilometers of shore and has a magnitude of about 20 m per month (La Fond 1966). Some of the most pronounced upwelling, of course, is found in the *eastern* portions of the mid-latitudinal oceans whereas the present theory gives intense vertical motion only near the western shore. This eastern upwelling is probably due to the persistent northerly winds near the eastern shore, which in turn induce a zonal temperature gradient near the coast; such effects have not been considered in the present solutions.

However, one possible comparison of the present theory is with the numerical solutions obtained by Bryan and Cox (1967) for vertical velocity beneath the Ekman depth. For the comparable latitutinal range (20°N to 60°N), the zonal stress,

$$\left.\begin{aligned} \tau_x^w &= -T\cos\left(\frac{2\pi y}{L}\right) \\ \tau_y^w &= 0, \end{aligned}\right\} \tag{65}$$

and the zonal surface temperature (61) are similar to those imposed by these authors; the stress (65) is a somewhat better approximation to the average conditions over midlatitudinal oceans than is (30). Under these conditions the solution of (60) is

$$\left.\begin{aligned} \eta(x,y) - \eta_0 = &-\frac{L^2 Q}{\pi^2}\sin\left(\frac{\pi y}{L}\right)\left[a_1 e^{b_1 x} + a_2 e^{b_2 x} - 1\right] - \\ &-\frac{L^2 P}{2\pi^2 \varrho_0 g}\sin\left(\frac{2\pi y}{L}\right)\left[m_1 e^{n_1 x} + m_2 e^{n_2 x} - 1\right], \end{aligned}\right\} \tag{66}$$

where the boundary height η_0 is given by

$$\eta_0 = \frac{2QL}{\pi^3}\left[\frac{a_1}{b_1}(e^{b_1 L} - 1) + \frac{a_2}{b_2}(e^{b_2 L} - 1) - L\right] \tag{67}$$

and where

$$n_{1,2} = -\frac{\gamma}{2} \pm \left[\left(\frac{\gamma}{2}\right)^2 + \left(\frac{2\pi}{L}\right)^2\right]^{1/2}, \tag{68}$$

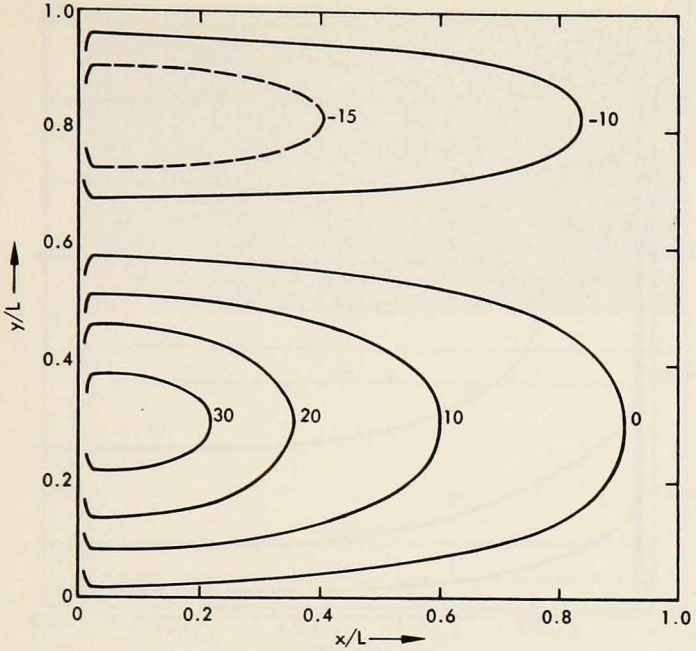

Figure 6. The distribution of surface elevation η in centimeters for a zonal wind stress $\tau^w{}_x = -T \cos(2\pi y/L)$ and zonal temperature $T_0(y) = \theta_0 - y(\Delta\theta/L) + (\Delta\theta/\pi) \sin(\pi y/L)$, with $T = 2$ dynes cm^{-2}, $L = 4000$ km, and $\Delta\theta = 20$ deg. The value on all boundaries is $\eta_0 = -9.1$ cm.

$$m_1 = (1 - e^{n_2 L})(e^{n_1 L} - e^{n_2 L})^{-1}, \tag{69}$$

$$m_2 = 1 - m_1. \tag{70}$$

This solution for water elevation is shown in Fig. 6 for the same constants used previously. Here the contribution of the surface temperature field (symmetric about $y/L = 0.5$) increased the magnitude of the elevated water in the southern half of the basin and correspondingly reduced the magnitude of the lowered water in the northern half; the result is a northward shift of the otherwise antisymmetric stress-induced elevation pattern.

With the solution of the simplified η-equation (60) known, we now return to (56) in order to determine the function W. With the approximation $E \ll H$ together with (60), we have

$$W = \frac{1}{\varrho_0 f} curl_z \pi^w - \frac{\beta g H}{f^2} \frac{\partial \eta}{\partial x} + \frac{\beta g \alpha E H}{8 f^2} \left(\frac{\partial T}{\partial y}\right)_0, \tag{71}$$

assuming $(\partial T/\partial x)_0 = 0$ as before. This relationship corresponds to (38) in the homogeneous case. For the imposed zonal temperature and stress fields

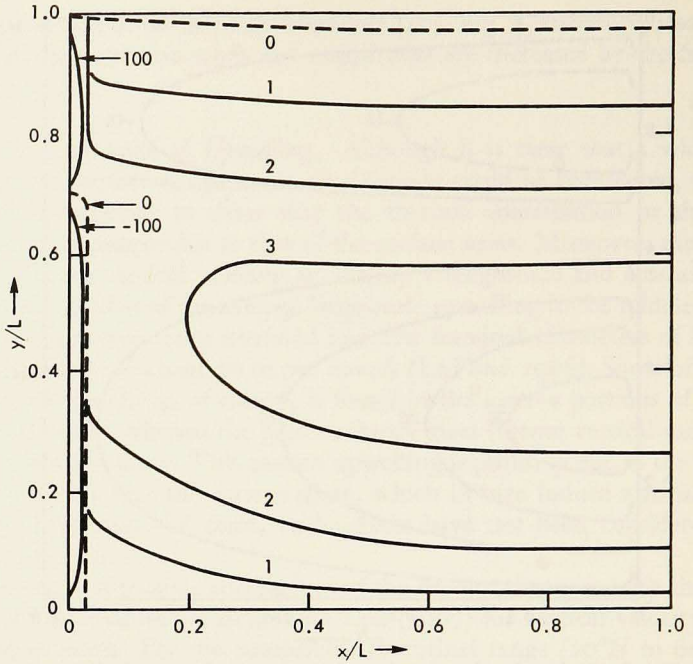

Figure 7. The distribution of vertical velocity $w_0 = W$ in 10^{-4} cm sec^{-1} at the top of the bottom boundary layer in an ocean subject to the zonal wind stress (65) and zonal temperature field (61), with $T = 2$ dynes cm^{-2}, $L = 4000$ km, and $\Delta\theta = 20$ deg. Significant sinking motion is found only near the western boundary, with a maximum of about 0.2 cm sec^{-1} at $x/L = 0, y/L = 0.31$.

(61) and (65) and from the solution (66), the distribution of W (the vertical motion at the top of the bottom boundary layer) is shown in Fig. 7. The β-induced westward intensification is again very marked, and the effect of the zonal surface temperature field is to produce a northward distortion of the pattern that would be expected from the zonal wind stress alone. With W and η now determined, we find from (54) the corresponding vertical motion w_1 at the base of the surface layer. With $(\partial T/\partial x)_0 = 0$ and $z \simeq H$, this leads to

$$w_1 = \frac{1}{\varrho_0 f} curl_z \pi^w + \frac{\beta g \alpha E H}{8 f^2} \left(\frac{\partial T}{\partial y}\right)_0. \tag{72}$$

This is a purely zonal distribution in the present approximation, with the thermal contribution here being about 10% of the stress-induced portion. The maxima of w_1 are -3.3×10^{-4}cm sec^{-1} and 3.0×10^{-4}cm sec^{-1}, approximately on the lines $y/L = 0.31$ and 0.81, respectively.

In order to compare the present results with those of Bryan and Cox (1967), we determine the vertical motion at the 200-m depth (the shallowest level for

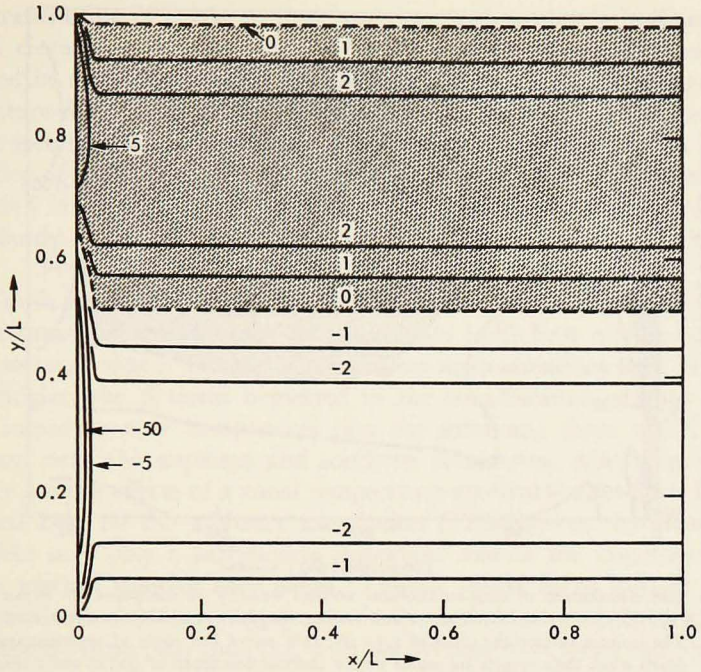

Figure 8. The distribution of vertical velocity in 10^{-4} cm sec^{-1} at a depth of 200 m, obtained by interpolation between the data in Fig. 7 (corresponding to $z = 0$ at the top of the bottom boundary layer) and those given by (72) (corresponding to $z = H = 4$ km at the base of the surface boundary layer). The shaded area is that of upward motion; the maximum downward motion is 1.0×10^{-2} cm sec^{-1} at $x/L = 0$, $y/L = 0.31$ (approximately).

which a solution is given by these authors). According to (54), with $(\partial T/\partial x)_0 = 0$, the interior vertical velocity varies linearly over depth between its distributions at $z = 0$ ($w = w_0 = W$) and $z = H$ ($w = w_1$); with $H = 4$ km, the w distribution at 200 m will therefore be given by $0.95\, w_1 + 0.05\, w_0$. This field is shown in Fig. 8; the near-equilibrium solution for comparable wind-forced and thermally forced motions at 200 m found by Bryan and Cox (1967) is shown in Fig. 9.

In the central portions of the basin, the large-scale distribution and magnitude of the vertical velocity is similar in both Figs. 8 and 9; the rising motion in the northern portion and the sinking motion in the southern portion of the basin are, in both solutions, essentially due to the dominance of the zonal wind-stress curl at this level. In the present linear solution (Fig. 8), the relatively narrow zone of intense vertical motion near the western wall is due to the westward intensification of the geostrophic β effect; the similar zone in Fig. 9 suggests that this effect is also important in the more complete numerical solution. However, note that Fig. 9 shows rising motion or upwelling along the entire western boundary, while Fig. 8 shows upwelling only along the

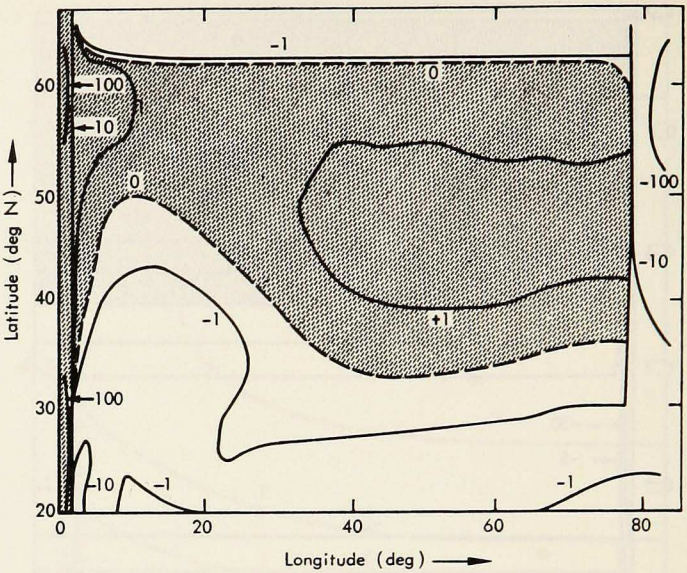

Figure 9. The distribution of near-equilibrium vertical velocity as computed by Bryan and Cox (1967), with a zonal wind stress and surface temperature similar to those used in Fig. 8. The isolines assume the units of 1.3×10^{-4} cm sec^{-1} and apply at approximately 200-m depth when their results are scaled with a thermocline depth of 400 m and a characteristic meridional temperature difference $\Delta\theta = 20$ deg. The shaded area is that of upward motion.

northern portion of this boundary. It is believed that this difference is due to the inclusion of lateral eddy viscous terms in the solution of Bryan and Cox. The principal contribution of these terms would be the creation of a viscous boundary layer along the western shore, where the vertical flux compensates that in the interior. The westward concentration in Fig. 8 is dependent upon the wind stress and only a vertical or Ekman eddy viscosity. From this point of view, the -10 isoline in Fig. 9 near the southwestern corner may be considered to correspond to the intense sinking motion in Fig. 8 along the southern part of the western wall.

Another significant comparison between Figs. 8 and 9 may be made along the northern portion of the eastern and western walls, and, to a lesser degree, along the northern boundary. In view of the argument used above, which hypothesizes a compensating flux in a western boundary layer dominated by lateral viscous effects, we would expect sinking motion close to the boundary on the northern part of the western wall where Fig. 9 shows strong rising motion. Therefore, the presence of lateral friction in the solutions of Bryan and Cox cannot account for this upwelling, nor can it account for the correspondingly intense downwelling in the northeastern part of the basin. These features are attributed by Bryan and Cox to a thermally-forced zonal convective motion in the northern portion of the basin; here the vertical temper-

ature stratification is nearly neutral, and deep overturning is facilitated. This thermal circulation is independent of the wind-induced motions and is not portrayed in the present linear theory, even with the addition of the surface temperature field. The temperature effect in the present model permits a more realistic specification of the surface boundary conditions (through an improved description of the velocity shear), but it does not simulate an independent thermal circulation in which the effects of vertical diffusion and temperature advection are evidently dominant (Robinson and Welander 1963, Bryan and Cox 1967).

7. *Concluding Remarks.* Although the present formulation may provide a useful estimate of the Ekman vertical velocity in at least middle latitudes, it is well to recall that a number of convenient approximations have been made. In particular, the β terms neglected in the simplification of (26) and (57) would introduce new components into the solutions; these would be most important near the northern and southern boundaries. Also of possible importance are the effects of a zonal temperature gradient; such effects have been neglected here by the arbitrary assumption $(\partial T/\partial x)_0 = 0$. In view of (54), this effect may play a particularly important role in the distribution of the interior vertical velocity over depth. Thus it would be of interest to obtain the vertical velocity from, say, (numerical) solutions of (57) for η and thence for W and w_I from (56) and (54), with the average wind stress and temperature fields imposed at the surface.

Another feature of the present solutions that warrants note is the presence of a net vertical flux over the basin. Except for rather special distributions of surface stress and temperature, the area integral of (24) or (55) over the basin will in general yield $\int_0^L \int_0^L W\,dxdy \neq 0$. With the lateral boundary condition $p = p_0$, this same nonzero vertical flux will be present not only at the top of the lower Ekman layer but at the base of the surface boundary layer and hence at each interior level as well. Therefore, even though we may balance the distributions of horizontal (geostrophic) velocity and mass through selection of the pressure or elevation boundary constant, there is evidently no way in which we can balance the vertical velocity flux in the present model.

Alternatively, if we balance the vertical flux by the arbitrary assignment of boundary conditions for W in the solution of, say, (29), then the solution of (26) for pressure could not be simultaneously applied and the kinematic boundary condition could not be enforced for the (geostrophic) interior motion. This paradox is apparently characteristic of a formulation in which the only dissipation is the vertical eddy viscosity acting in the surface and bottom boundary layers. It is believed that this defect can be removed by the introduction of lateral eddy viscosity in a new lateral boundary layer just outside the p = constant "wall" of the present formulation. As noted earlier, such a model would permit a more realistic comparison with the upwelling computations of Bryan and Cox (1967). This extension will be reported in a future paper.

REFERENCES

BRYAN, KIRK, and M. D. COX
1967. A numerical investigation of the oceanic general circulation. Tellus, *19*: 54–80.

EKMAN, V. W.
1905. On the influence of the earth's rotation on ocean currents. Ark. Math. Astr. Fys., *2*: 1–52.
1923. Über horizontal zirkulation bei winderzeugten meeresströmungen. Ark. Math. Astr. Fys., *17*: 1–74.

LAFOND, E. C.
1966. Upwelling. *In* Encyclopedia of Oceanography, pp. 957–959. Ed., R.W. Fairbridge. Reinhold, New York. 1021 pp.

ROBINSON, A. R.
1965. Oceanography. *In* Research Frontiers in Fluid Dynamics, pp. 504–533. Ed., R. J. Seeger. Interscience, New York. 738 pp.

ROBINSON, A. R., and PIERRE WELANDER
1963. Thermal circulations on a rotating sphere with application to the oceanic thermocline. J. mar. Res., *21*: 25–38.

STOMMEL, HENRY
1948. The westward intensification of wind-driven ocean currents. Trans. Amer. geophys. Un., *29*: 202–206.
1956. On the determination of the depth of no meridional motion. Deep-sea Res., *3*: 273–278.

SVERDRUP, H. U.
1947. Wind-driven currents in a baroclinic ocean; with application to the equatorial currents of the eastern Pacific. Proc. nat. Acad. Sci., *33*: 318–326.

WELANDER, PIERRE
1957. Wind action on a shallow sea: some generalizations of Ekman's theory. Tellus, *9*: 45–52.

YOSHIDA, KOZO, and H.-L. MAO
1957. A theory of upwelling of large horizontal extent. J. mar. Res., *16*: 40–54.